Anharmonic effects and Faust-Henry coefficient of CdTe in the vicinity of the energy gap

V. C. Stergiou,[1] A. G. Kontos,[1,2] and Y. S. Raptis[1]
[1]*Physics Department, School of Applied Mathematical and Physical Sciences, National Technical University of Athens, Zografou Campus, GR-157 80 Athens, Greece (EU)*
[2]*Institute of Physical Chemistry, NCSR "Demokritos," Aghia Paraskevi Attikis, 153 10 Athens, Greece (EU)*
(Received 1 October 2007; revised manuscript received 17 March 2008; published 3 June 2008)

Crystallodynamic properties of CdTe are studied, by Raman spectroscopy, as a function of the temperature and excitation energy. The temperature dependence (in the range of 20–300 K) of the peak frequency and the full width at half maximum of the Raman scattering bands, which were obtained from the $q \approx 0$ optical (LO and TO) lattice vibrations, are mainly attributed to the anharmonic effects due to the phonon decay toward the $q \neq 0$ points of the Brillouin zone. The intensity ratio (LO/TO) of the phonons is also studied as a function of the temperature and excitation energy, leading to a Faust-Henry coefficient that is nearly constant over the energy range investigated (1.49–1.54 eV).

DOI: 10.1103/PhysRevB.77.235201 PACS number(s): 71.55.Gs, 78.30.−j, 63.20.Ry

I. INTRODUCTION

CdTe is a zinc blende type semiconducting material of the II–VI group with a direct energy gap in the infrared range (1.49–1.59 eV) and it is an appealing candidate for several optoelectronic applications that rely on its interesting electronic,[1–3] crystallodynamic,[4–8] and piezoelectric[9–11] properties. Specifically, CdTe, as well as the $Cd_{1-x}M_xTe$ ternary compounds (where M is a metal, e.g., Zn, Mn, Hg), is a key material for gamma and x-ray detectors,[12] solar cells,[13] laser windows, and electro-optic modulators. Furthermore, CdTe can be potentially incorporated in electronic structures, glass matrices, or solution precipitations in the form of quantum dots or nanorods,[14] the size of which determines their absorbance and luminescence properties, with various applications in microelectronics, optics, and biology.

Despite the intensive studies on the various physical properties of CdTe during the last decades (see above), there are physical aspects of the material that either have not been investigated at all or need further confirmation by complementary experimental methods, in addition to the results recently appearing in the literature. An important parameter to be explored is the Faust-Henry coefficient (FHC), $C = e^*/M\omega_T^2[(\partial\chi/\partial u)/(\partial\chi/\partial E)]$, which is of basic, as well as of technological, interest since it is a measure of the relative contribution (to the linear susceptibility χ) of the deformation potential coupling $(\partial\chi/\partial u)$ to the electro-optical mechanism $(\partial\chi/\partial E)$; e^*, M, and ω_T are the transverse effective charge, the reduced mass, and the frequency of the transverse optical phonon, respectively. As far as we know, the value (C) for CdTe, in the frequency range close to its energy gap, has not been unquestionably, published up to now. From early data on the LO/TO intensity ratio,[15] it can be deduced that the Faust-Henry coefficient shows a nonlinear dispersion from −0.15 to −0.8 in the excitation-energy range of 1.50–1.56 eV. On the other hand, a value of $C=-0.5$, which was deduced via the relation $C=(d_{41}^{EO}/d_{41}^{E})-1$ (Ref. 16) by the electronic part of the nonlinear electro-optic coefficient $(d_{41}^{EO}=36.4$ pm/V) and the second harmonic generation coefficient $(d_{41}^{E}=73$ pm/V) at 0.83 eV (Ref. 17) (i.e., far below the low-T fundamental energy gap of CdTe at 1.59 eV), does not fall on the tendency of the above mentioned dispersion.

At the same time, the temperature dependence of the phonon characteristics of CdTe and the associate anharmonic analysis is also missing from literature with the exception of a quite recent work,[18] wherein the fundamental (TO) and the higher-order phonon–phonon interactions are studied through the temperature dependence of the dielectric function. This investigation, however, is carried out at a frequency range covering the 2TA(X) critical point but with an upper limit by ~50% lower than the frequency range of the optical-phonon branches. Consequently, the above work does not concern direct measurements of the TO phonon but is an indirect calculation of the frequency and damping rate through measurements of the absorption and refractive index spectra in different temperatures. As a result of this work, there is only a brief discussion of the anharmonic effects while the main result is the calculation of the effective charge.

In the present paper, we present a systematic Raman study of CdTe under different temperatures (22–300 K) and excitation energies (1.49–1.54 eV). The analysis of the Raman measurements leads to results related to the anharmonic effects, as well as to the calculation of FHC. The study of anharmonic behavior, which leads to the separation of the phonon-decay (direct) and the volume-expansion (indirect) effects, is done in the lines of several previous studies concerning the anharmonic effects in molecular,[19–21] ionic,[22–25] as well as mixed ionic-covalent[26–28] crystals. The FHC, on the other hand, is related to the intensity ratio of optical phonons (LO/TO). The study of the FHC as a function of temperature and excitation energy shows the change in the scattering efficiency when both the deformation potential and the electro-optic mechanisms are affected.

This paper is organized as follows: Section II describes the experimental conditions. In Sec. III, (a) the experimental results are presented, (b) the temperature dependence of the phonon frequency shifts and linewidths are analyzed by the anharmonic effects of the material, and (c) the FHC is determined as a function of temperature and excitation energy. In Sec. IV, all of the above issues are discussed in comparison to the corresponding results obtained in other III–V and

II–VI semiconductors while some general trends are presented.

II. EXPERIMENTAL DETAILS

The undoped CdTe samples used in this work were rectangular single crystal plates (provided by Keystone Crystal Corporation) with typical dimensions of a few millimeters and with faces used for backscattering geometry of either (110) or (001) crystallographic orientation. Fine polishing of the samples and Raman experiment configurations were carefully conducted under the same conditions for different samples in order to obtain reliable data from the Raman scattering.

The Raman spectra were excited with a Ti:sapphire laser (Spectra-Physics, 3900S) pumped by an argon ion laser (Spectra-Physics, Stabilite 2017). An excitation beam with a power from 30 to 120 mW (depending on the experiment) was focused on the scattering face by a spherical lens of 75 mm focal length. The power level, in combination with the excitation-beam spot diameter (>40 μm), ensures the minimalization of the laser heating effects. For the anharmonic-analysis data, unpolarized (both incident and scattered radiations) spectra have been measured in order to record both LO and TO bands since intensities were not taken into account in this analysis. For the Faust-Henry coefficient calculations, parallel and perpendicular polarization orientations were used for the incident and the scattered light with respect to the crystallographic orientations [001] and [110], as it is described below [see Sec. III C] and in the discussion related to Eq. (6), (as well as in Ref. 40, therein). The scattered light was analyzed by a SPEX 1403 double spectrometer and detected by a cooled photomultiplier tube (C31034 RCA), and the spectra were recorded by standard photon-counting methods. The temperature was controlled by using a closed-circle He cryostat (CCC1104 Oxford Instruments).

For the anharmonic analysis, the backscattering Raman spectra were measured along the [110] direction. For this direction, the selection rules impose scattering only from the TO phonons. However, deviation from the selection rules also leads to scattering from the LO phonon. This is due to the resonance effects since the Ti:sapphire laser emits in the range of the CdTe energy gap.

The excitation energies varied from 1.537 to 1.454 eV while the temperature was changed from 22 to 300 K. The initial excitation energy at 22 K has been chosen so that both optical-phonon types appear in the spectra. The appropriate energy region to achieve that is 775.2–826.5 nm (12 900–12 100 cm^{-1}). Outside this region, either the luminescence background was strong enough to cover the TO phonon or the excitation energy is quite far from the energy gap, preventing the resonance phenomena to appear. Furthermore, for the accurate determination of the phonon linewidths, the slit size was kept very low and progressively reduced at low temperatures, allowing less than 10% of overestimating error.

For the calculation of the FHC, Raman backscattering of the Raman scattering was performed along the [110] direction where TO phonons are "allowed," while the Raman spectra that was obtained by backscattering along the [001] direction produced LO phonons, in accordance to the selection rules. The measured spectra were further corrected for the finite width of the spectrometer resolution function,[29] that is, a triangular function for the specific wave number range and slits' width. The measurements were carried out either at constant temperature 22 K, by varying the excitation wavelength, or by varying the temperature. For the measurements with an increasing temperature, we have decreased the excitation energy in such a way as to follow the corresponding temperature dependence of the energy gap and keep the same near-resonance conditions, allowing a standard 64 meV difference between the excitation and the band gap energies. The exact temperature dependence of the energy gap was determined by using photoluminescence measurements, which were initially performed down to 22 K. An $E_g(T) = E_g(0) - S\hbar\omega[\coth(\hbar\omega/kT) - 1]$ dependence was estimated with $\hbar\omega = 6.24$ meV, $E_g(0) = 1.591$ eV, and $S = 4.904$, in accordance to Ref. 30.

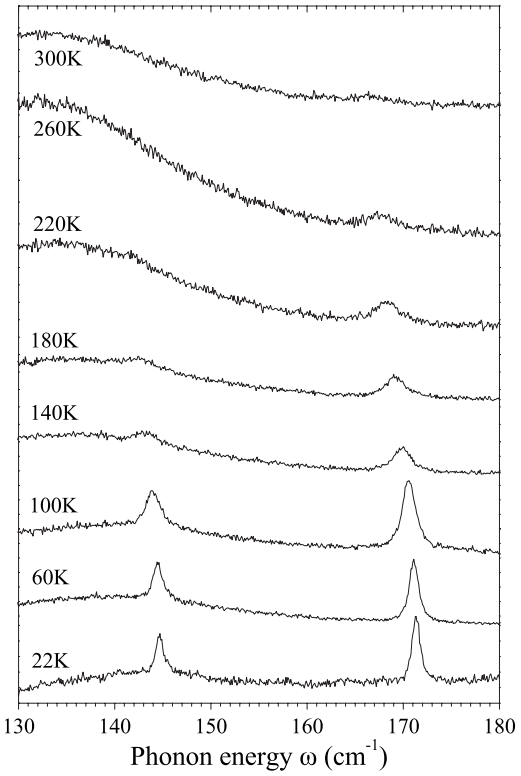

FIG. 1. Unpolarized Raman backscattering spectra along [110] of bulk CdTe at various temperatures. The excitation energies used for recording the spectra sequentially from bottom to top were 1.537, 1.537, 1.537, 1.500, 1.488, 1.475, 1.463, and 1.454 eV.

III. RESULTS AND ANALYSIS

A. Raman spectra

In order to study the anharmonic effects, Raman backscattering at near resonance conditions was performed along the [110] direction. In Fig. 1, the characteristic Raman spectra are shown for the two types of phonons acquired at different temperatures.

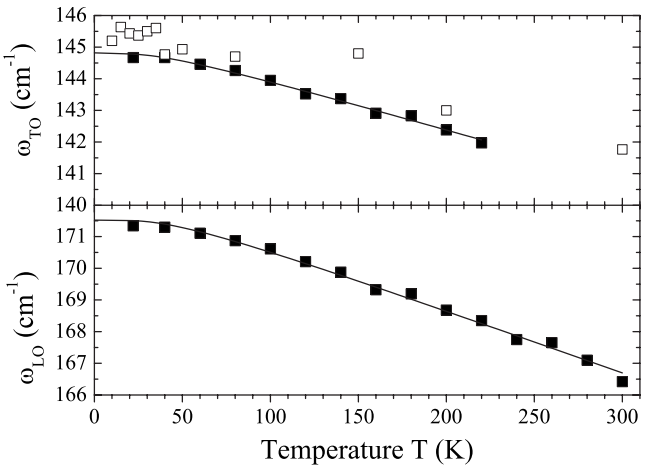

FIG. 2. Temperature dependence of the experimentally obtained LO and TO Raman frequencies (full squares) of CdTe. The solid lines are polynomial fits. The TO data from Ref. 18 are also shown (open squares).

Similar spectra that were measured with the variable excitation energy show no significant changes, as it will be shown below (calculation of the Faust-Henry coefficient by the LO/TO intensity ratios). By increasing the temperature, the phonon frequencies (energies) of the two modes decrease, their full widths at half maximum (FWHMs) increase, while their intensities decline because of phonon-decay mechanisms. Above 200 K, the TO Raman peak is hardly resolved due to the luminescent background increase. Phonon frequencies vs temperature for the LO and TO modes are shown in Fig. 2 as full squares. The data are fitted with second-order polynomial curves (solid lines) with zero-temperature TO and LO frequencies $\omega(0)$ that were predicted to be equal to 144.8 and 171.4 cm^{-1}, respectively. In Fig. 2, the TO frequencies from Ref. 18 (open squares) are also shown for comparison.

B. Anharmonic analysis

The above results are used for the anharmonic analysis of CdTe. In the case of an ideal crystal, the shape of the scattering zone is a delta (δ) function, while in the case of a real crystal, the shape of the scattering zone is described by a symmetric Lorenzian curve. The width of this curve is due to the lifetime of the phonons (τ), i.e., the time until the phonons decay, via anharmonicity. This effect is temperature dependent and arises from the decay of phonons from the center of the Brillouin zone into combinations of phonons with a zero total wave number and a total frequency that is equal to the zero-temperature frequency (as a consequence of energy and momentum conservation).

1. Raman shifts

While a phonon frequency is primarily determined by the harmonic part of the vibrational potential energy, its variation with temperature is entirely determined by the anharmonic part.[31] A change in temperature, in addition to the effect on the vibrational amplitudes of the atoms about their equilibrium positions (direct-explicit effect), also alters the interatomic spacing (indirect-implicit effect) because of volume expansion, which in turn, affects the bond force constants.[20] The contribution to the phonon frequencies can be deconvolved and separately studied for explicit ($\Delta\Omega_{\text{temperature}}$) and implicit ($\Delta\Omega_{\text{volume}}$) effects. Following the thermodynamic considerations, we have

$$\frac{d\omega}{dT} \equiv \left(\frac{\partial\omega}{\partial T}\right)_V - \frac{\beta}{\kappa}\left(\frac{\partial\omega}{\partial P}\right)_T, \tag{1}$$

where $\beta \equiv (1/V)(\partial V/\partial T)_P$ is the volume thermal expansion coefficient, $\kappa \equiv -(1/V)(\partial V/\partial P)_T$ is the volume compressibility, and $\gamma \equiv (1/\kappa\omega)(\partial\omega/\partial P)_T$ is the Grüneisen parameter, which is different for the TO and the LO mode. Thereafter, the contribution of the volume expansion to the frequency shift $\Delta\Omega_{\text{volume}}(T)$ can be directly calculated by integration of the implicit second term in Eq. (1),

$$\Delta\Omega_{\text{volume}}(T) = -\int_0^T \frac{\beta}{\kappa}\left(\frac{\partial\omega}{\partial P}\right)_T dT' \tag{2a}$$

$$= -\gamma\int_0^T \beta\omega dT' \tag{2b}$$

$$\approx -\omega(0)\gamma\int_0^T \beta dT'. \tag{2c}$$

In the calculations below, we have used Eq. (2b), which holds under the assumption that $\gamma^{T(L)}$ are pressure independent and are constant over the temperature range of the experiment. This approximation results in a simple $\omega \sim V^{-\gamma}$ relation between the frequency and volume, and it is applied to 3D covalent crystals,[32] such as semiconductors of the groups IV, III–V, and II–VI, where $\gamma^{T(L)}$ is on the order of unity. The values $\gamma^T = 1.61$ and $\gamma^L = 1.01$ are known from the CdTe literature.[33] It should be mentioned that, at this point, instead of Eq. (2b), either Eq. (2a), under the assumption of a constant $d\omega/dP$ slope, or even the simple form in Eq. (3), which assumes further that $\omega(T) \approx \omega(0)$, could be used. The results of the calculations with different methods are very similar.

Now, regarding the temperature dependence of the volume thermal expansion coefficient β, it is deduced by the experimental values of the linear thermal expansion coefficient $\alpha(T) = \beta(T)/3$ at temperatures of 0–35 and 300 K (Ref. 7), as well as between 55–100 K (Ref. 6). Negative α values at low temperatures are common in semiconductors [also found, for example, in ZnSe (Ref. 34)]. The literature results are plotted in Fig. 3 and fitted by the following expression:

$$\beta(T) = \left(\frac{E}{T} - \frac{F}{T^2}\right)\sinh^{-1}\left(\frac{G}{T}\right), \tag{3}$$

where the E, F, and G constants are equal to $(1.14 \pm 0.04) \times 10^{-3}$, $(69.1 \pm 2.8) \times 10^{-3}$ K, and $(65.85 \pm 0.98) \times 10^{-3}$ K, respectively. Although $\beta(T) = (E/T - F/T^2)\sinh^{-2}(G/T)$ is the relation that was used for the best fit in previous studies,[35] this was not possible in our case because of the negative values of β in the low temperature range. Nevertheless, the numerical fit to the experimental data is reasonably good, as

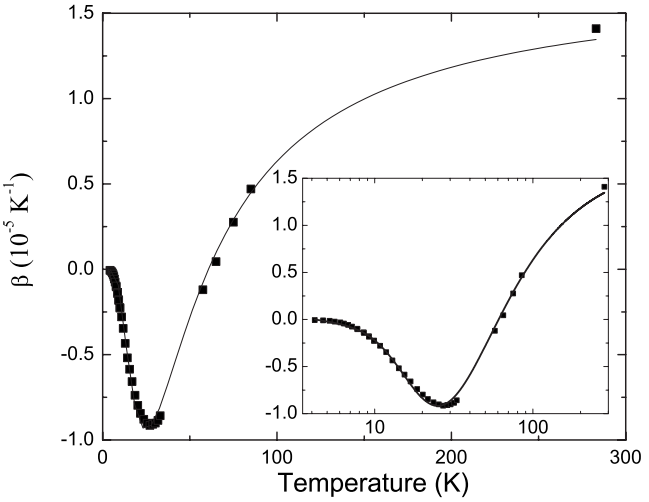

FIG. 3. Volume thermal expansion coefficient β of CdTe for various temperatures 0–300 K. The data points are results from literature (Refs. 6 and 7). The line fit according to Eq. (3) is shown. The inset (in logarithmic temperature scale) is added to confirm the fitting quality and elucidate the range of deviation from the experimental data.

it can be seen from Fig. 3 and from its inset (wherein a logarithmic temperature scale is used in order to better clarify the slight deviation of the numerical fitting in the reproduction of the experimental data minimum).

The integral of Eq. (3) for each temperature (T) is calculated by using . The calulated "volume contribution" frequency shifts from Eqs. (2b) and (3) and the polynomial of Fig. 2, are shown with solid lines in Fig. 4. When the implicit effect is known, the explicit effect on the phonon frequency shifts can be merely determined by subtracting the indirect from the experimentally observed total Raman shifts. This is done in Fig. 4, which presents the corrected LO and TO phonons shifts (data in symbols). The anharmonicity theory

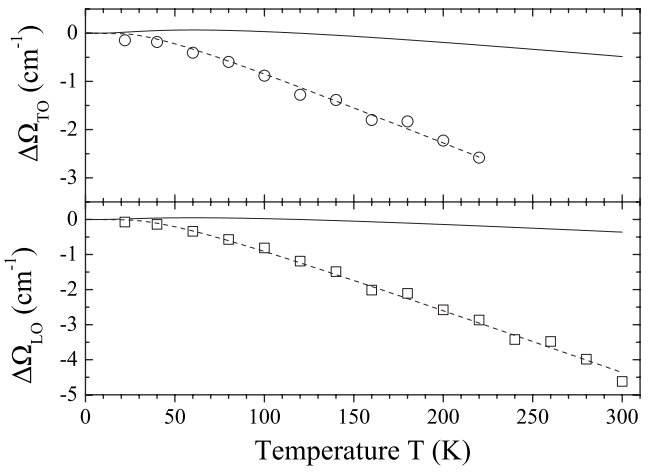

FIG. 4. The calculated volume-expansion contribution to the TO and LO anharmonic frequency shifts of CdTe are shown by the solid lines. The Raman shifts calculated from the data in Fig. 2, after the correction for the implicit effect, are shown by the symbols. The dashed lines are fits of the corrected shifts (explicit temperature effect) to Eq. (4), with c as a free parameter and $d=0$.

TABLE I. Fitting parameters that were deduced from the temperature dependence of the anharmonic phonon frequency shifts $[\omega(0),c]$ and linewidths (Γ_0,a) for CdTe. ZnSe results (Ref. 38 and Appendix) are shown for comparison.

	$\omega(0)$ (cm^{-1})	c (cm^{-1})	Γ_0 (cm^{-1})	a (cm^{-1})
TO(CdTe)	144.8	-0.78 ± 0.10	0.18 ± 0.10	0.91 ± 0.15
LO(CdTe)	171.4	-1.11 ± 0.05	0.16 ± 0.05	0.88 ± 0.10
LO(ZnSe)	259.5	-0.94 ± 0.05		0.67

that comprises of three- or four-phonon processes[36,27] predicts that the remaining shift $\Delta\Omega(T)$ is equal to

$$\Delta\Omega(T) = c(1+2n_2) + d(1+3n_3+3n_3^2) - c - d$$
$$= \Delta\Omega_{\text{temperature}}(T) - c - d, \quad (4)$$

where n_2 and n_3 are the statistical Bose–Einstein numbers $\{n=[\exp(\hbar\omega/kT)-1]^{-1}\}$ of the phonons at the frequencies $\omega(0)/2$ and $\omega(0)/3$, and c and d are constants, which represent the contributions in $\Delta\Omega_{\text{temperature}}(T)$ from the phonon decay in two or three phonons, respectively. The last constant term secures a zero shift at 0 K and it has to be added to $\Delta\Omega(T)$ for counting the total explicit $\Delta\Omega_{\text{temperature}}(T)$ effect. The corrected $\Delta\Omega(T)$ data in Fig. 4 have been fitted according to Eq. (4) by considering only the first bracket term in the equation, which is dominant in the temperature range of the experiment. Fitting with the complete form does not significantly improve the quality of the fit, whereas the error of d is bigger than the deduced value itself.

In conclusion, the anharmonic analysis ascertains a small volume contribution in the phonon frequency shift despite the polar character of the material, which is a fact that is explained in Sec. IV. The value of the fitting parameter c, together with the corresponding one for ZnSe (see the Appendix), is shown in Table I.

2. Linewidths

In Fig. 5, we present the temperature dependence of the FWHMs of the TO and LO phonon peaks in the Raman spectra (full squares), wherein, TO bandwidths from literature (see Ref. 18; open squares) are also shown for comparison. As it is evident, the direct estimation through the Raman spectra leads to FWHMs smaller by a factor of two in comparison to the ones indirectly obtained by the conventional terahertz time-domain method since the frequency range considered (in the terahertz studies) does not include the whole bands. The experimental Raman data for the widths are omitted when their error bars are on the order of magnitude of the FWHM. According to the anharmonic theory, the temperature dependence of the linewidths for phonons, which decay into two or three phonons, is

$$\Gamma(T) = \Gamma_0 + a(1+2n_2) + b(1+3n_3+3n_3^2), \quad (5)$$

where a and b are constants with the same physical meaning as c and d, and Γ_0 is a constant that represents any residual broadening due to lattice imperfections.[37]

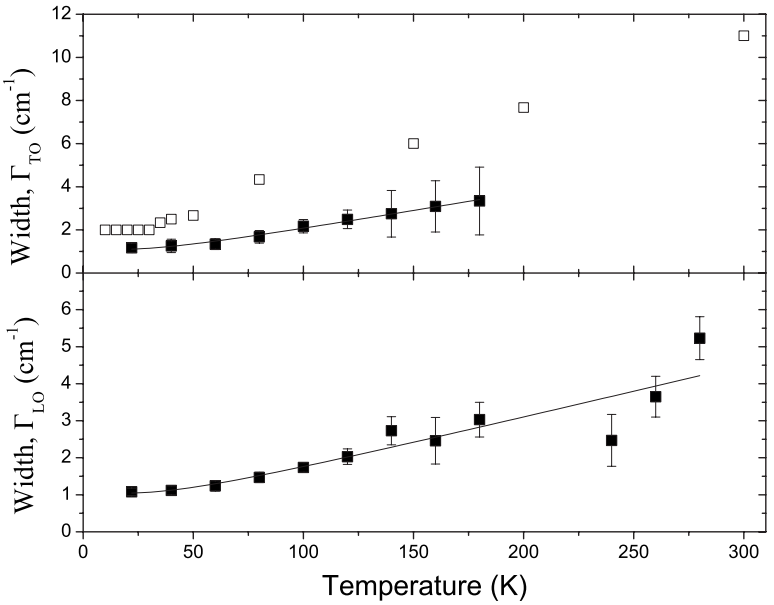

FIG. 5. Temperature dependence of the FWHMs of the LO and TO phonon peaks (full squares). The missing data are due to big errors. The lines represent the fittings according to Eq. (5) with free parameters Γ_0 and a, and $b=0$. The TO data from Ref. 18 are also shown (open squares).

As it was done for the shifts, the FWHM data points are also fitted only with the first term of Eq. (5). The deduced values of a are given in Table I and compared well to those found for the ZnSe LO mode.[38]

From the linewidth, the TO- and LO-phonon lifetimes can be deduced by the $\tau(\text{ps})=100/[3\pi\Gamma(\text{cm}^{-1})]$ relation. Accordingly, $\tau_{LO}=12.0\pm1.4$ ps and $\tau_{TO}=11.7\pm1.9$ ps are predicted at 0 K, and $\tau_{LO}=2.3\pm0.3$ ps at 300 K. The last value is well above that (0.75 ps) obtained by transient picosecond Raman spectroscopy.[39] Apparently, measuring the phonon lifetimes is very sensitive to the presence of defects in the crystal and to the experimental method used.

C. Faust-Henry coefficient

The Faust-Henry coefficient (C) expresses the ratio of the lattice to the electronic contribution in the linear electro-optic tensor. Experimentally, it can be calculated via the ratio (ρ_{exper}) of the scattering efficiency by LO (lattice and electronic contribution) to the scattering efficiency by TO (only lattice contribution) phonons[40] as follows:

$$C=\left(\frac{\omega_{LO}^2-\omega_{TO}^2}{\omega_{TO}^2}\right)\left\{1-\left[\left(\frac{n_{TO}+1}{n_{LO}+1}\right)\left(\frac{\omega_{TO}^S}{\omega_{LO}^S}\right)^4\left(\frac{\omega_{LO}}{\omega_{TO}}\right)\times\left(\frac{\rho_{expt}}{\rho_{theor}}\right)\right]^{1/2}\right\}^{-1}, \quad (6)$$

where $\omega_{LO,TO}$ are the LO and TO phonon frequencies, $\omega_{LO,TO}^S$ are the Stokes scattering frequencies, $n_{LO,TO}$ are the LO and TO Bose–Einstein occupation numbers, and ρ_{theor} is the ratio of the Raman-tensor elements, LO/TO, according to the selection rules, where only the scattering geometry, incident and scattered light polarizations, and symmetry considerations (in the form of the appropriate Raman-tensor elements) are taken into account.

In Fig. 6(a), we present the calculated dependence of C on the excitation energy on the base of our Raman data for values lower than the CdTe energy gap (1.591 eV) at 22 K. In Fig. 6(b), we show the temperature dependence of C. The corresponding measurements were taken by changing the excitation energy E_x, with temperature, in such a way that the difference between E_x and the energy gap remain constant in order to keep it at the same level against any resonance effects. Two different data sets were deduced by the experimental ratio of the LO intensity from the intensity of the two differently polarized TO phonons [conventionally denoted as TO_V and TO_H, meaning vertically ($\perp$ [001]) and horizontally ($\parallel$ [001]) polarized TO phonons, respectively]. The two sets did not show any systematically different behavior. Concerning the energy dependence of the Faust-Henry coefficient C,

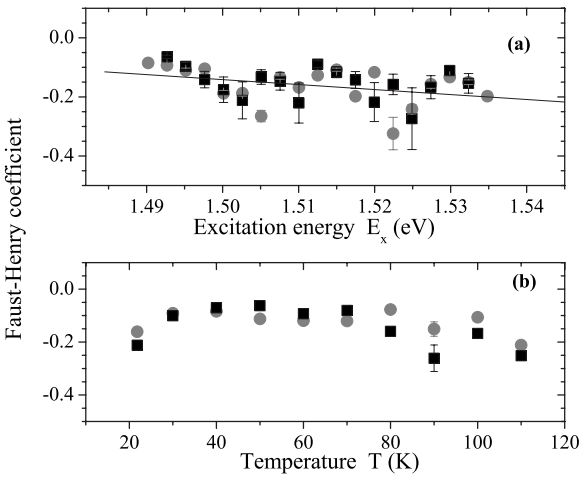

FIG. 6. (a) Energy (at $T=22$ K) and (b) temperature (with $E_g-E_x=64$ meV) dependences of the Faust-Henry coefficient that were deduced from the intensity ratio of the LO over any of the two degenerate TO phonons alternatively oscillating with either perpendicular (circles) or parallel (squares) polarization, relative to the [001] axis. In (b), the representative error bars were drawn only for one point of each data group. Similar or lower errors apply to all other data points. The apparent variation vs energy is discussed in Sec. III C (see text). The solid line is a linear fit of the energy dispersion data.

as it is displayed in Fig. 6(a), there is a tendency of an oscillation as a function of energy. One can estimate the approximate periodicity in the energy scale in the order of (1525–1505 meV)=20 meV, i.e., $\approx$160 cm^{-1}, which is close to the average frequency of the optical phonons [e.g., using the data of ω_0 from Table I, $(\omega_{TO}+\omega_{LO})/2 \approx 158\ cm^{-1}$]. This correlation might suggest resonance phenomena with optical-phonon replicas. However, the variation is on the order of magnitude of the error bar, as shown in Fig. 6; therefore, such an attribution is considered as rather risky. It is decided, consequently, to simply take the average C value, with an almost negligible energy dependence, as it is shown below. The results of the calculations according to Eq. (6) yielded a mean value of $C=-0.14\pm0.12$. This mean value does not disagree with the results deduced from Ref. 15, although the data of the present work show no significant dispersion in the energy range examined, in contrast to the former ones. Our data imply a very weak energy dispersion of C, ($\approx -1.5\ eV^{-1}$; see below, in Sec. IV), while an increase in the temperature up to 120 K does not affect it. In the past, negative FHC values that lie in between 0 and −0.7 have been found for all semiconducting materials of the groups III–V and II–VI.[41] Negative values of C are also theoretically predicted by Flytzanis in Ref. 42.

IV. DISCUSSIONS AND CONCLUSIONS

Models[43] that describe the anharmonic behavior of covalent crystals do not take into account the Coulomb interatomic forces; hence, they cannot be adapted in the case of piezoelectric crystals. An alternative way of looking at the relative importance of the two contributions (temperature and volume) is to calculate the *implicit factor n* (ratio of the volume to the total effect[44]),

$$n = \frac{\Delta\Omega_{volume}(T)}{\Delta\Omega_{volume}(T) + \Delta\Omega_{temperature}(T)}. \quad (7)$$

The implicit factor value of a material is usually correlated to its crystal type,[44] specifically in the following ways:

(a) Values lower than 0.5 indicate a covalent crystal or internal modes in molecular crystals. In this case, there is a charge overlap between the vibrating units.

(b) Values near unity indicate ionic crystals or external modes in molecular crystals. In this case, the vibrations involve relative motions of electronically nonoverlapping closed-shell entities.

(c) Values higher than unity indicate opposite sign contributions from the two effects (implicit and explicit) or the cancellation of the two effects if the factor becomes infinite.

The calculated temperature dependence of the implicit factor for the two optical phonons of CdTe is shown in Fig. 7. Despite the ionic character of the material, the factor takes very small values near zero for both the TO and the LO modes in the whole 0–300 K temperature range. Below 120 K, it is negative, while by increasing the temperature, it presents a tendency to increase and reach a flat level. The results

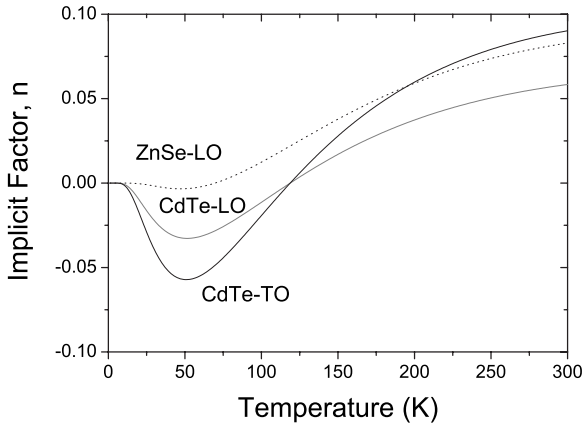

FIG. 7. Temperature dependence (0–300 K) of the implicit factor (n), for the two optical phonons (LO, TO) of CdTe and the LO of ZnSe.

of the temperature dependence of the implicit factor for the ZnSe LO phonon mode are shown for comparison as well. The calculations for ZnSe are presented in the Appendix. The two materials have similar electronic configurations (Cd:[Kr]$4d^{10}5s^2$ and Te:[Kr]$4d^{10}5s^25p^4$, and Zn:[Ar]$3d^{10}4s^2$ and Se:[Ar]$3d^{10}4s^24p^4$) and similar fractional ionic characters [0.685 for CdTe (Ref. 45) and 0.63 for ZnSe].

Generally, the assumption of a significant contribution in anharmonicity from the implicit effects is based on the existence of electronically nonoverlapping closed-shell entities,[44] which is characteristic of ionic compounds. In our case, CdTe is a mixed ionic-covalent crystal; consequently, it is questionable which of the two mechanisms, i.e., the volume expansion or the phonon decay, dominates the Raman shift vs temperature. Despite that, the implicit factor n is well below 0.5 and resembles the one found in Si ($n=0.1$ at RT[46]), which has the [Ne]$3s^2p^2$ electronic structure and purely covalent character. The above tendency for n is also found for ZnSe (see Fig. 7), as well as various copper halides,[28] which have a large fractional ionic character[45] as well.

Apparently, the various semiconducting compounds present a very small implicit factor independent of the partially ionic character of the bonding. This might be due to the electronic structure of the materials, which form the tetrahedrally coordinated zinc blende structure. Accordingly, d orbitals might play an important role in the clear description of the bonding, as well as in the atomic interactions. It would be interesting, therefore, to confirm this possibility by means of theoretical calculations supported by independent experimental evidence from other compounds.

As far as the FHC is concerned, we can see that C is almost temperature independent while the dependence of C on the excitation energy, according to our data, is very small ($\Delta C_V/\Delta E_X=-1.7\pm1.0\ eV^{-1}$, $\Delta C_H/\Delta E_X=-1.4\pm1.1\ eV^{-1}$). This fact denotes a balance between deformation potentials (due to the lattice deformation) and the electro-optic contribution (due to the longitudinal vibrations)[41] at the phonon scattering process. Indeed, for excitation-photon energies located lower than the energy gap, there is *a priori* no reason for C to exhibit strong dispersive effects. The tendency of C

to get increasing negative values when approaching the energy gap (negative $\Delta C/\Delta E_x$ slopes) reflects the gradual strengthening of the electro-optic contribution. Our poor correlation to the previous data,[15,17] concerning the value and the energy dispersion of the Faust-Henry coefficient, needs further elucidation.

Concerning the comparison of the temperature dependence of the phonon characteristics (peak position and bandwidth), as it is deduced either by Raman or by conventional terahertz time-domain spectroscopy,[18] it is obtained that the Raman scattering yields more reliable results, at least as far as the terahertz measurements do not cover the whole frequency range corresponding to the TO phonons. Actually, while the temperature dependence of the TO-frequency induced by the two methods is almost the same with the Raman data exhibiting a less noisy tendency, the TO-bandwidth obtained by the Raman method shows a weaker temperature dependence, which we claim as more reliable with respect to the ones indirectly obtained by the terahertz measurements.

In conclusion, we have studied by using Raman spectroscopy the anharmonic effects of CdTe through the temperature dependence of the frequencies and widths of the TO and LO phonons in the frequency range right below the energy band gap. Despite the ionic character of the material, the volume contribution to the anharmonicity is fairly small. This behavior is probably common for all semiconductors with a diamond or zinc blende structure. The Faust-Henry coefficient was determined to be equal to -0.14 ± 0.12 in the whole temperature and energy range of the experiment, and in accordance to the corresponding values in other semiconductors.

ACKNOWLEDGMENTS

We acknowledge partial financial support by the Basic-Research program "THALES" of NTUA.

APPENDIX

1. Anharmonic analysis of the LO phonon frequency shifts in ZnSe

For the anharmonic analysis of the LO frequency shifts in ZnSe, we have used the results of Ref. 38 and corrected it for the implicit effect in the same way as it was done for CdTe. The data of the volume-expansion coefficient at various temperatures[34] were fitted with a similar formula to Eq. (3) with -1.2 as the power of the sinh function, i.e., $\beta(T) = (E/T - F/T^2)\sinh^{-1.2}(G/T)$, and $E = 0.69 \times 10^{-3}$, $F = 0.0336$ K, and $G = 96.6$ K.

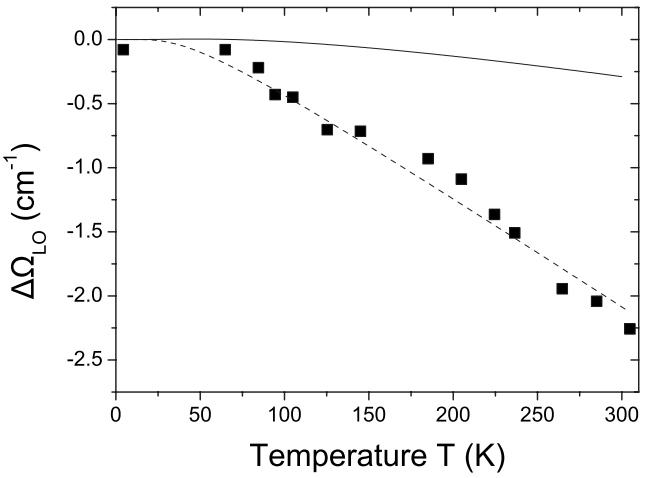

FIG. 8. Calculated volume contribution to the total LO Raman shift of ZnSe (solid line). The corrected data of Ref. 38 are shown and fitted (dashed line), according to the anharmonic temperature first bracket term in Eq. (4).

The calculated volume contribution to the total shift is shown in Fig. 8 together with the corrected Raman shifts. These data account for the temperature contribution to the shift and have been fitted to Eq. (4), resulting in c equal to -0.94 (see Table I). The small c value justifies the nearly linear dependence of the LO Raman frequencies of the isotopic modified ZnSe samples on $\mu^{-1/2}$, where μ is the ZnSe reduced mass.[47] Otherwise, a significant shift to the higher energies would be observed.[48] The results for the calculated temperature dependence of the implicit factor are shown in Fig. 7.

[1] M. Cardona and D. L. Greenaway, Phys. Rev. **131**, 98 (1963).
[2] A. D. Brothers and J. B. Brungardt, Phys. Status Solidi B **99**, 291 (1980).
[3] P. Hiesinger, S. Suga, F. Willmann, and W. Dreybrodt, Phys. Status Solidi B **67**, 641 (1975).
[4] A. Nakamura and C. Weisbuch, Solid State Commun. **32**, 301 (1979).
[5] P. Plumelle and M. Vandevyver, Phys. Status Solidi B **73**, 271 (1976).
[6] R. D. Greenough and S. B. Palmer, J. Phys. D **6**, 587 (1973).
[7] T. F. Smith and G. K. White, J. Phys. C **8**, 2031 (1975).
[8] D. J. Dunstan, B. Gil, and K. P. Homewood, Phys. Rev. B **38**, 7862 (1988).
[9] R. André, C. Deshayes, J. Cibert, Le Si Dang, S. Tatarenko, and K. Saminadayar, Phys. Rev. B **42**, 11392 (1990).
[10] A. Dal Corso, R. Resta, and S. Baroni, Phys. Rev. B **47**, 16252 (1993).
[11] V. C. Stergiou, N. T. Pelekanos, and Y. S. Raptis, Phys. Rev. B **67**, 165304 (2003).
[12] T. Kishishita, H. Ikeda, T. Kiyuna, K. I. Tamura, K. Nakazawa, and T. Takahashi, Nucl. Instrum. Methods Phys. Res. A **580**, 1363 (2007); R. Franchi, F. Glasser, A. Gasse, and J. C. Clemens, *ibid.* **563**, 249 (2006); E. Saucedo, V. Corregidor, L. Fornaro, A. Cuna, and E. Dieguez, Thin Solid Films **471**, 304 (2005).
[13] M. Burgelman, in *Thin Film Solar Cells*, edited by J. Poortmans and V. Arkhipov (Wiley, New York, 2007), p. 277–314.
[14] R. Osovsky, V. Kloper, J. Kolny-Olesiak, A. Sashchiuk, and E.

Lifshitz, J. Phys. Chem. C **11**, 10841 (2007); Y. Lei, C. Y. Jiang, S. J. Liu, Y. M. Miao, and B. S. Zou, J. Nanosci. Nanotechnol. **6**, 3784 (2006).
[15] M. Selders, E. Y. Chen, and R. K. Chang, Solid State Commun. **12**, 1057 (1973).
[16] S. Zekeng, B. Prevot, and C. Schwab, Phys. Status Solidi B **150**, 65 (1988).
[17] E. Bocchi, A. Milani, A. Zappettini, S. M. Pietralunga, and M. Martinelli, Synth. Met. **124**, 257 (2001).
[18] M. Schall, M. Walther, and P. U. Jepsen, Phys. Rev. B **64**, 094301 (2001).
[19] E. Sarantopoulou, Y. S. Raptis, E. Zouboulis, and C. Raptis, Phys. Rev. B **59**, 4154 (1999).
[20] R. Zallen and M. L. Slade, Phys. Rev. B **18**, 5775 (1978).
[21] P. S. Peercy, G. A. Samara, and B. Morosin, J. Phys. Chem. Solids **36**, 1123 (1975).
[22] A. Perakis, E. Sarantopoulou, Y. S. Raptis, and C. Raptis, Phys. Rev. B **59**, 775 (1999).
[23] S. S. Mitra, C. Postmus, and J. R. Ferraro, Phys. Rev. Lett. **18**, 455 (1967).
[24] J. A. Taylor, M. S. Haque, J. E. Potts, J. B. Page, Jr., and C. T. Walker, Phys. Rev. B **12**, 5969 (1975).
[25] P. S. Peercy and B. Morosin, Phys. Rev. B **7**, 2779 (1973).
[26] Y. S. Raptis and E. Anastassakis, Solid State Commun. **76**, 335 (1990).
[27] Y. S. Raptis, G. A. Kourouklis, E. Anastassakis, E. Haro-Poniatowski, and M. Balkanski, J. Phys. (Paris) **48**, 239 (1987).
[28] H. D. Hochheimer, M. L. Shand, J. E. Potts, R. C. Hanson, and C. T. Walker, Phys. Rev. B **14**, 4630 (1976).
[29] A. K. Arora and V. Umadevi, Appl. Spectrosc. **36**, 424 (1982).
[30] G. Fonthal, L. Tirado-Mejía, J. I. Marín-Hurtado, H. Ariza-Calderón, and J. G. Mendoza-Alvarez, J. Phys. Chem. Solids **61**, 579 (2000).
[31] I. P. Ipatova, A. A. Maradudin, and R. F. Wallis, Phys. Rev. **155**, 882 (1967).
[32] This approximation is not valid for molecular crystals, wherein several types of bonds are present, grouping the vibrational modes in internal (intramolecular) and external (intermolecular) ones. In the case of tetrahedral crystals, there are some differences depending on the phonon type, as well as between crystals with different degrees of homo- or heteropolarity (see Ref. 44).
[33] A. K. Arora, D. U. Bartholomew, D. L. Peterson, and A. K. Ramdas, Phys. Rev. B **35**, 7966 (1987); The experimental value for the TO Grüneisen parameter was obtained by H.-M. Karaya and T. Soma, Phys. Status Solidi B **138**, K13 (1986).
[34] *Physics of II-VI and I-VII Compounds, Semimagnetic Semiconductors*, Landolt-Bornstein, New Series, Group III, Vol. 17, Pt. B, edited by O. Madelung and M. Schulz (Springer, New York, 1982).
[35] E. Liarokapis, E. Anastassakis, and G. A. Kourouklis, Phys. Rev. B **32**, 8346 (1985).
[36] M. Balkanski, R. F. Wallis, and E. Haro, Phys. Rev. B **28**, 1928 (1983).
[37] B. Bairamov, Yu. E. Kitaev, V. K. Negoduiko, and Z. M. Khashkhozhev, Fiz. Tverd. Tela (Leningrad) **16**, 2036 (1974)[Sov. Phys. Solid State **16**, 1323 (1975)].
[38] L. Y. Lin, C. W. Chang, W. H. Chen, Y. F. Chen, S. P. Guo, and M. C. Tamargo, Phys. Rev. B **69**, 075204 (2004).
[39] E. Grann, Y. Chen, K. T. Tsen, D. K. Ferry, T. Almeida, Y. P. Chen, J. P. Faurie, and S. Sivananthan, J. Appl. Phys. **80**, 3840 (1996).
[40] A. Anastassiadou, Y. S. Raptis, and E. Anastassakis, J. Appl. Phys. **60**, 2924 (1986).
[41] M. Cardona, in *Light Scattering in Solids II*, Topics in Applied Physics Vol. 50, edited by M. Cardona and G. Güntherodt (Springer, Berlin, 1982), p. 19.
[42] C. Flytzanis, Phys. Rev. B **6**, 1264 (1972).
[43] E. L. Slaggie, Phys. Rev. B **2**, 2230 (1970).
[44] B. A. Weinstein and R. Zallen, in *Light Scattering in Solids IV*, edited by M. Cardona and G. Güntherodt (Springer-Verlag, Berlin, 1984), p. 463.
[45] Y. Al-Douri, R. Khenata, Z. Chelahi-Chikr, and M. Driz, J. Appl. Phys. **94**, 4502 (2003).
[46] H. Tang and I. P. Herman, Phys. Rev. B **43**, 2299 (1991).
[47] A. Göbel, T. Ruf, J. M. Zhang, R. Lauck, and M. Cardona, Phys. Rev. B **59**, 2749 (1999).
[48] J. Serrano, M. Cardona, T. M. Ritter, B. A. Weinstein, A. Rubio, and C. T. Lin, Phys. Rev. B **66**, 245202 (2002).